Journal of Engineering and Technology for Industrial Applications

ISSN ONLINE: 2447-0228

ITEGAM-JETIA

Manaus, v.12 n.58, p.1072-1083. March/April, 2026.
DOI: https://doi.org/10.5935/jetia.v12i58.3258

RESEARCH ARTICLE OPEN ACCESS

RESPONSE SURFACE METHODOLOGY-BASED OPTIMIZATION OF INJECTION TIMING AND HYDROGEN FLOW IN AN MAHUA BIODIESEL–HYDROGEN DUAL-FUEL ENGINE

Kumaran P*[1], Sathiyaraj S[2], Vijayakumar K[3], Manivannan.M[4] and Rajasekar. R[5]

[1, 2, 3,4,5]Department Mechanical Engineering, Aarupadai Veedu Institute of Technology, Vinayaka Mission's Research Foundation (deemed to be university), Salem, Tamilnadu, India.

[1]http://orcid.org/0000-0003-2781-8999, [2]http://orcid.org/0000-0001-8504-0412, [3]http://orcid.org/0000-0002-5964-982X
[4]http://orcid.org/0009-0009-9160-9287, [5]http://orcid.org/0009-0002-5859-4158

Email: *kumaranp@avit.ac.in, sathiyaraj@avit.ac.in, vijayakumar@avit.ac.in, mahendranmani208@gmail.com and r.rajasekar_rajesh@yahoo.in

ARTICLE INFO

Article History
Received: January 8, 2026
Reviewed: February 10, 2026
Accepted: March 22, 2026
Published: April 30, 2026

Keywords:
Mahua biodiesel,
Hydrogen blend,
Dual-fuel engine,
Variable compression ratio,
Response Surface Methodology,
Brake thermal efficiency.

ABSTRACT

Investigations on alternative diesel engine fuels have intensified due to the growing demand for cleaner energy sources. This study adopts a novel methodology by examining the performance, combustion, and pollutant emissions of a single-cylinder, four-stroke variable compression ratio engine fueled by an M25 biodiesel-hydrogen dual-fuel blend, with optimal injection timing in conjunction with hydrogen enrichment. The subsequent injection timings and hydrogen flow rates evaluated were IT21, IT24, IT27, and IT30 degrees prior to TDC. Under full load conditions, IT30 operating with a hydrogen flow rate of 16 lpm attained a minimum brake-specific fuel consumption (BSFC) of 0.28 kJ/kWh and a maximum brake thermal efficiency (BTE) of 32.7%. The experimental settings elevated the cylinder pressure by 11.7 % and the heat release rate by 8 % relative to usual operation. The emission investigation results indicated a 54% reduction in carbon monoxide (CO), a 24.7% reduction in hydrocarbons (HC), and a 37.2% reduction in smoke opacity; nevertheless, due to elevated combustion temperatures, NOx emissions increased by 7.2% to 820 ppm. The ideal working condition, as determined by Response Surface Methodology optimization is IT30.25˚ and 16 lpm H2. This design forecasts a BTE of 32.52% and NOx emissions of 790 ppm. Statistical validation was accomplished by diagnostic methods, and this study introduces an innovative methodology that combines biodiesel combustion enhancement with meticulous regulation of hydrogen flow and timing adjustments. M25-hydrogen blends demonstrate potential as a viable decarbonized engine technology, with a performance-enhanced approach to satisfy BS-VI and Euro VI standards.

I. INTRODUCTION

The growing demand for sustainable energy solutions has driven significant interest in alternative fuels for compression ignition engines. Dual-fuel strategies offer a pathway to reduce fossil fuel dependence and emissions while maintaining acceptable performance levels. Achieving optimal results requires precise control and optimization of key engine parameters. Mahua biodiesel, produced and characterized optimized blend with water and diethyl ether (DEE) by RSM. Optimum: 15.23% MB, 15% water, 15% DEE as per ASTM standards. Validation showed better performance, lower emissions, and 45% fossil fuel reduction [1]. Mahua biodiesel transesterification were optimize using hybrid RSM–GA. As per ASTM standards, this work confirming mahua oil's potential as a cost-effective biodiesel source [2]. Castor, mahua, and dairy waste oils were mixed (1:1:1) for biodiesel by RSM–CCD optimization. Optimum levels were attained at: 2.82% catalyst, 63.93°C, 7.86:1 methanol:oil, yield 95.91% (94% exp.). The proposed research shows as low-cost and eco-friendly feedstock [3]. solar still with chimney and condenser submerged in ocean water was studied. Modified still improved output by 9.1%, yielding 6.2 L/m²·day vs 5.3 for simple still. Efficiency gains attributed to better convection and condensation [4].

Crude sunflower–mahua oil biodiesel by esterification–transesterification was optimized. Using Plackett–Burman design (PBD), Box–Behnken design (BBD) and generalized reduced gradient (GRG), achieved 93.34% FFA conversion at 3.52% FFA, 8.61 molar ratio, 1.45% catalyst at 63.9°C. Suggested CSMO as viable biodiesel feedstock [5]. Waste cooking oil 50% (WCOB50)–diesel blends with hydrogen (4–8 lpm) in a dual-fuel CI engine was investigated. WCOB50 showed negligible BTE drop compared to diesel; hydrogen addition improved combustion and reduced emissions. Tests confirmed viability of WCO blends with hydrogen induction for sustainable fuel use [6]. The study evaluated injection timing (19°, 23°, 27°, and 31° BTDC) with B20–hydrogen blends (20–25 lpm) in a DI diesel engine, finding that the optimum setting of 27° BTDC with 22.5 lpm H_2 achieved the highest BTE (24.4–34.3%), lowest BSFC and minimal HC/CO emissions, while advancing or retarding the timing reduced efficiency but lowered NOx emissions [7]. HCCI mode with hydrogen and Mahua oil methyl ester (MOME) combined with EGR was investigated to reduce smoke and NOx emissions, and it was found that H_2–MOME blends enhanced thermal efficiency and overall emission performance in CI engines, thereby demonstrating the potential of renewable fuels for sustainable engine operation [8].

A deep learning pipeline was developed to detect and classify culvert blockages using the VHD and ICOB datasets, where Mask R-CNN achieved 77.2% mAP@75 in segmentation and NASNet attained 81.2% classification accuracy, demonstrating its applicability for real-time blockage monitoring [9]. Acetylene (LRF) with B20 MOME (HRF) was tested in RCCI mode by varying the injector position (243.5–333.5 mm from the valve), with the optimal placement at 243.5 mm yielding a 2.27% increase in BTE and reductions in EGT and NOx by approximately 13.5%, demonstrating that injector positioning is critical for performance and emissions [10]. Mahua biodiesel–biogas dual-fuel was used in a diesel engine and optimized using RSM for compression ratio and load, achieving a BTE of 15.25%, a liquid fuel replacement of 68.9%, and low emissions of NOx (39 ppm) and HC (90 ppm). Validation confirmed that the predicted and experimental results matched within a 6% error margin [11]. A counterflow double-pipe heat exchanger was tested using TiC and CNT nanofluids in alkaline water, and at 0.06 vol% particle concentration with constant velocity, the nanofluids exhibited superior heat absorption compared to water, with the enhanced thermal properties improving the exchanger's efficiency [12]. B10 biodiesel–water–Al_2O_3 nanoparticle blends were studied in a single-cylinder CI engine, with B10W8N100 improving BTE by 7.6–10.72% and reducing CO emissions by up to 24.4% compared to B10. The catalytic effect of Al_2O_3 enhanced combustion and lowered NO emissions by 50% relative to diesel [13].

Mahua biodiesel production was optimized through esterification (H_2SO_4, 4.2%) and transesterification (Na-methoxide, 2.2%), and tested on a single-cylinder CI engine across varying loads. Higher biodiesel content was found to lower BTE and increase SFC, while emissions varied across the different blends [14]. Diesel–mahua–waste palm biodiesel–t-butyl peroxide blends were assessed with injection timings of 21–25° bTDC, with D50-MB20TB30 at 25° reducing CO, HC, and smoke by approximately 3–5% compared to diesel, while NOx increased by 0.83%. The heat release rate and cylinder pressure were found to be slightly lower than those of diesel [15]. Biodiesel from mahua, mango seed, and pongamia was investigated in a low-heat rejection CI engine with lanthanum oxide coatings and l-ascorbic acid additive. The coated engines exhibited higher performance and reduced NOx emissions, demonstrating the viability of eco-friendly fuel use in coated CI engines [16]. Mahua oil methyl ester was produced by esterification and transesterification with process parameters optimized using Box–Behnken RSM. The highest yield (92%) was achieved at a 6:1 methanol-to-oil ratio, 1% KOH, 60 °C, and 120 min. Fuel properties complied with ASTM standards, and GC–MS along with FTIR analyses confirmed the formation of fatty acid methyl esters [17]. A mahua shell–derived heterogeneous catalyst was used for two-step mahua biodiesel production with process optimization by BBD–RSM yielding 87.7% at a 14.88 molar ratio, 3.578% catalyst loading, 69.7 °C, and 81.9 min.

Diesel simulation confirmed the process's sustainability and demonstrated favorable performance and emissions characteristics [18]. Biodiesel was synthesized from pongamia–mahua mixed oils using in-situ KOH derived from K_2CO_3 in NH_4OH, with process parameters optimized by RSM. A maximum yield of 96.5% was achieved at 1.5 g K_2CO_3, 0.75 g NH_4OH, a 7:1 molar ratio, 55 °C, and 75 min. GC–MS, ^1H NMR, and FTIR analyses confirmed the successful conversion to esters [19]. A CI aero piston engine was studied at altitudes ranging from 10 to 1920 m using pressure simulation, revealing that higher altitude reduced intake flow, thermal efficiency, and peak pressure, while increasing ignition delay, combustion duration, NOx, HC, and smoke emissions. CO emissions increased at low and high loads but remained stable at medium load [20]. Methane–diesel dual-fuel operation was investigated with an optimum injection timing of 11°CA bTDC at MEF levels of 0–50%, where methane reduced NO emissions by up to 67% and smoke by 82%, but increased HC and CO at low to medium loads. Exhaust energy loss was improved by 13.5%, indicating that high methane substitution is a promising approach [21]. This research will illuminate the combustion dynamics of biodiesel and hydrogen, paving the way for cleaner, more efficient fuel alternatives for diesel engines.

II. MATERIALS AND METHODS

The performance and emission characteristics of M25 biodiesel blends at varying hydrogen flow rates were examined utilizing a variable compression ratio (VCR) engine, four-stroke, single-cylinder. This study selected a variable compression ratio (VCR) engine due to its capability for precise adjustment of the compression ratio (CR), hence optimizing combustion parameters across diverse dual-fuel operating conditions. The ability to adjust the compression ratio without a preset setting provides a unique advantage for evaluating the effects of biodiesel-hydrogen blends on performance and emissions. The utilization of a VCR engine provided greater flexibility for future research, despite the compression ratio being consistent across all test scenarios to isolate the impacts of injection timing and hydrogen enrichment. The VCR system is a commendable choice for dual-fuel optimization studies because to its inherent adaptability, which facilitates improved flame propagation, efficient atomization, and superior in-cylinder thermodynamic performance. The Kirloskar TV1 engine sustained a constant speed of 1500 rpm during the testing period. The engine specifications utilized in the experiment have now been provided to enhance clarity and reproducibility. It utilized a Kirloskar-manufactured Variable Compression Ratio (VCR) diesel engine, characterized by a single cylinder, four-stroke design, and water cooling. The following are the paramount details: Bore of 87.5 mm, stroke of 110 mm, rated output of 5.2 kW at 1500 rpm, with an adjustable compression ratio ranging from 12:1 to 18:1. A piezoelectric pressure transducer and crank angle encoder were fitted in the engine for combustion study, and an eddy current dynamometer was attached for load variation.

These standards ensure a standardized and regulated framework for evaluating the performance of biodiesel-hydrogen dual-fuel engines with varying injection timings. The tested fuels were M25 mixtures with different hydrogen concentrations: M25+3H2, M25+6H2, M25+9H2, and M25+12H2. A calibrated flow meter was employed to supply hydrogen to the intake manifold as part of a dual-fuel injection strategy, ensuring precise control of the hydrogen delivery. To ensure a consistent flow and composition for the dual-fuel trials, the hydrogen gas employed in this study was procured from a commercial industrial gas supplier in high-purity cylinders, with a purity of 99.99%. The target flow rates of 3, 6, 9, and 12 lpm were attained by maintaining high-pressure storage and employing precise flow controls for regulation. An AVL 444 gas analyzer was put in the engine arrangement to measure emissions, including CO, HC, NOx, and smoke opacity. Particle emissions were quantified with an AVL smoke meter. Employing a piezoelectric pressure transducer, we recorded the internal pressure of the cylinder and utilized that data to compute the heat release rate. The integration of the data acquisition system (DAQ) with IC Engine Soft software facilitated real-time combustion analysis. The impact of hydrogen enrichment on combustion efficiency was assessed by measuring the brake specific fuel consumption (BSFC) at different brake mean effective pressures (BMEP). M25+3H2 had a BSFC of 0.67 kJ/kWh at 1.256 bar, whereas M25+9H2 demonstrated a reduced value of 0.55 kJ/kWh, indicating that the use of hydrogen improved fuel efficiency. Table 1 enumerates the attributes of the fuel.

Table 1: Fuel properties for varying injection timings and different hydrogen flow rates.

Fuel property	**M25 + $3H_2$ (IT30)**	**M25 + $6H_2$ (IT30)**	**M25 + $9H_2$ (IT30)**	**M25 + $12H_2$ (IT30)**	**M25 + $12H_2$ (IT24)**	**M25 + $12H_2$ (IT27)**	**M25 + $12H_2$ (IT30)**	**M25 + $12H_2$ (IT33)**
Density (kg/m^3)	885	883	881	879	883	881	879	877
Kinematic viscosity (mm^2/s@40°C)	4.2	4.1	4	3.9	4.1	4	3.9	3.8+
Calorific value (MJ/kg)	41.5	41.7	42	41.9	40.2	42.2	42.5	42.7
Cetane number	52	53	55	56	54	55	56	57
Flash point (ºC)	73	72	70	67	71	69	67	65
Fire point (ºC)	78	76	74	72	76	74	72	70
Cloud point (ºC)	8	7.5	7	6	7	6.5	6	5.5
Pour point (ºC)	-1	-2	-3	-4	-2	-3	-4	-5
Latent heat of vaporization (kJ/kg)	250	253	258	265	255	260	265	270
Stoichiometric air-fuel ratio	14.4	14.5	14.7	14.8	14.6	14.7	14.8	14.9

Source: Authors, (2026).

Variations in injection timings (IT) induced minor yet discernible alterations in the characteristics of the fuel mixture during premixed combustion dynamics. The cetane number and latent heat of vaporization were influenced by variations in apparent fuel reactivity and ignition characteristics when the injection timing transitioned from IT21 to IT30. In the M25+12H2 combination, the cetane number incrementally rose from 53 to 57, while the viscosity diminished from 4.1 to 3.6 mm^2/s as the IT advanced. Enhancements in atomization and mixing during subsequent injection timings account for these alterations, resulting in finer droplet formation and improved combustion start. The results of pulverization are influenced by alterations in physical and thermal properties caused by injection phasing. Experimental measurements of the base fuel (M25 biodiesel) and estimations for the hydrogen component, employing established thermodynamic concepts, were utilized to ascertain the characteristics of the dual-fuel blends. A range of injection timings (IT21, IT24, IT27, and IT30) was examined in greater depth to assess their impact on BSFC, BTE, EGT, CO, HC, NOx, smoke, cylinder pressure, ignition delay, and HRR. Comprehensive data on the combustion, performance, and emission characteristics of dual-fuel operation was obtained from the experimental study of M25 biodiesel with hydrogen enrichment and varying injection timings. The findings indicate that the use of hydrogen enhances combustion efficiency, reduces emissions, and improves engine performance, all while maintaining the engine at optimal temperature. The results indicate the potential of utilizing biodiesel supplemented with hydrogen as a more environmentally friendly fuel for compression ignition engines.

III. RESULT AND DISCUSSIONS

III.1 SPECIFIC FUEL CONSUMPTION (SFC)

Figure 1 illustrates the performance and combustion characteristics of M25 fuel blended with hydrogen at flow rates of 3, 6, 9, and 12 lpm. It also illustrates the variation of the acronyms BSFC, BTE, and EGT with engine load. The enhanced combustion efficiency resulting from elevated in-cylinder temperatures and pressures leads to a reduction in the BSFC of all blends as the load increases. The BSFC of M25+12H2 is the lowest overall, decreasing from 0.68 kJ/kWh at 1.25 kW (M25+3H2) to 0.54 kJ/kWh, a decline of 20.6%, and from 0.30 kJ/kWh to 0.26 kJ/kWh at full load, a drop of 13.3%. Lower hydrogen flow rates result in less cycle-to-cycle fluctuations and incomplete combustion, while enhanced diffusivity, broader flammability limits, and accelerated flame speeds in hydrogen contribute to improved combustion and expedited ignition.

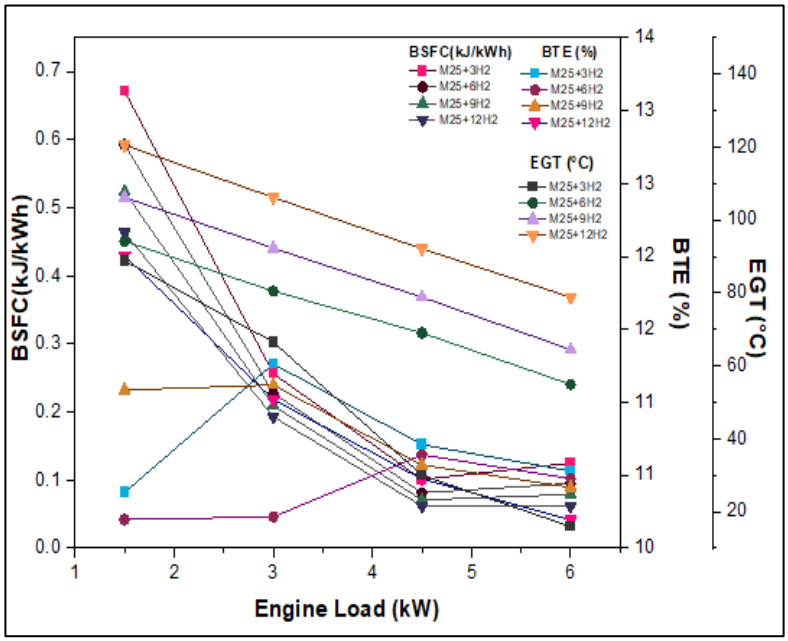

Figure 1: BSFC, BTE & EGT with varying engine loads.
Source: Authors, (2026).

Likewise, BTE increases with load for both blends; however, M25+12H2 surpasses M25+3H2 due to accelerated combustion initiation, reduced ignition delay, and more complete oxidation of the mixture; this disparity is 14.2% at 1.25 kW (24.2% improvement) and 32.5% at 5.0 kW (10.2% enhancement). Hydrogen enrichment results in a decrease in exhaust gas temperature (EGT) as load increases, due to more efficient combustion that converts a greater amount of energy into usefsul work while producing less residual heat in the exhaust. This contrasts with the observation that EGT rises with load for all mixes due to increased fuel injection and combustion energy release. The improvement in combustion efficiency, thermal management, and overall engine performance in dual-fuel operation is evidenced by the concurrent trends in BSFC, BTE, and EGT, indicating that an increase in hydrogen flow enhances these parameters. In another study, ethanol fumigation (15%) evaluated with Exhaust gas recirculation (EGR) (0–20%) in PCCI diesel engine at 2–4 bar BMEP. Ethanol + EGR reduced NOx and smoke, with slight BTE gain at moderate/high load. BSFC and ignition delay rise; CO and HC decreased moderately in ER15EGR0 vs diesel [22].

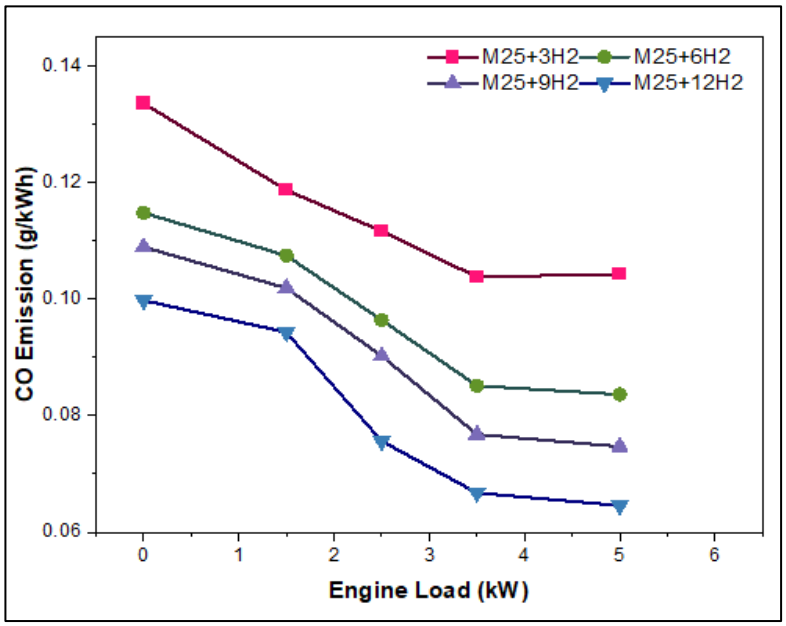

Figure 2: CO emission with varying engine loads.
Source: Authors, (2026).

Figure 2 illustrates the carbon monoxide emissions for M25 gasoline combined with hydrogen at flow rates of 3, 6, 9, and 12 lpm, while varying engine loads. A discernible trend indicates a reduction in CO emissions with increasing engine load, which becomes significantly more pronounced at elevated hydrogen concentrations. M25+12H2 emits approximately 0.105 g/kWh at 0 kW load, representing a 25% decrease in CO emissions relative to M25+3H2, which produces around 0.14g/kWh. The gap is accentuated at maximum load (5.0 kW), with M25+3H2 recording 0.10 g/kWh and M25+12H2 declining to 0.06 g/kWh, indicating a 40% reduction.

Decreased hydrogen flow (3 lpm) results in incomplete combustion due to ineffective fuel-air premixing and insufficient flame propagation, thereby increasing CO emissions. Reduced loads, especially with constrained hydrogen assistance, result in combustion temperatures and in-cylinder pressures that are insufficient for the complete oxidation of carbon content. Conversely, carbon monoxide production diminishes by enhancing combustion efficiency and optimizing local stoichiometry with elevated hydrogen mixtures. In previous studies, mahua biodiesel with nano metal oxides evaluated in a BSII single-cylinder diesel engine. Aluminium oxide improved BTE, reduced ignition delay, and normalized fuel consumption to diesel levels. Achieved lower HC, CO_2, CO, and NOx emissions at varying loads [23].

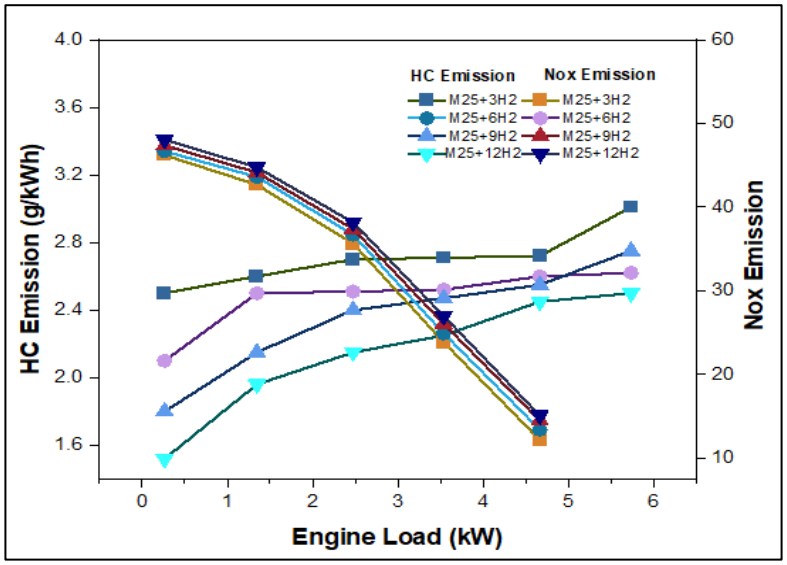

Figure 3: HC emission and NOx Emission with varying engine loads.
Source: Authors, (2026).

Figure 3 illustrates the correlation between engine load and the variability of unburned hydrocarbon (HC) and nitrogen oxide (NOx) emissions from M25 fuel blended with hydrogen at flow rates of 3, 6, 9, and 12 lpm. Increased hydrogen enrichment markedly decreases hydrocarbon emissions, which escalate with load across all blends, indicating that hydrogen enhances combustion and reduces incomplete oxidation. Due to enhanced flame propagation and reduced quenching zones at elevated hydrogen flow rates, HC emissions diminish from 3.25 g/kWh to 1.75 g/kWh at full load (5.0 kW), and from 3.25 g/kWh for M25+3H2 to 3.1 g/kWh for M25+12H2 at zero load, representing a 36% reduction. Conversely, NOx emissions also rise with load due to elevated in-cylinder temperatures and pressures; yet, while exhibiting lower combustion efficiency, M25+3H2 consistently generates the highest NOx levels, measuring 500 ppm at maximum load, in comparison to 400 ppm for M25+12H2 (a 20% variance). This ostensibly paradoxical tendency stems from the postponement and prolongation of combustion with less hydrogen concentration, which promotes the formation of nitrogen oxides (NOx) through post-flame oxidation and extended residence times at elevated temperatures. Enhanced combustion phasing, expedited ignition, and diminished high-temperature exposure due to increased hydrogen flows result in decreased CO and HC emissions and mitigated NOx production. The findings indicate that in dual-fuel operation, optimal hydrogen enrichment is essential for maximizing efficiency and minimizing emissions during combustion. In earlier study, a CRDI engine tested with mahua methyl ester (MME100) under varying fuel injection pressures. Higher pressure (1000 bar) improved BTE by 12.33%, reduced smoke, CO, and HC emissions due to better atomization [24].

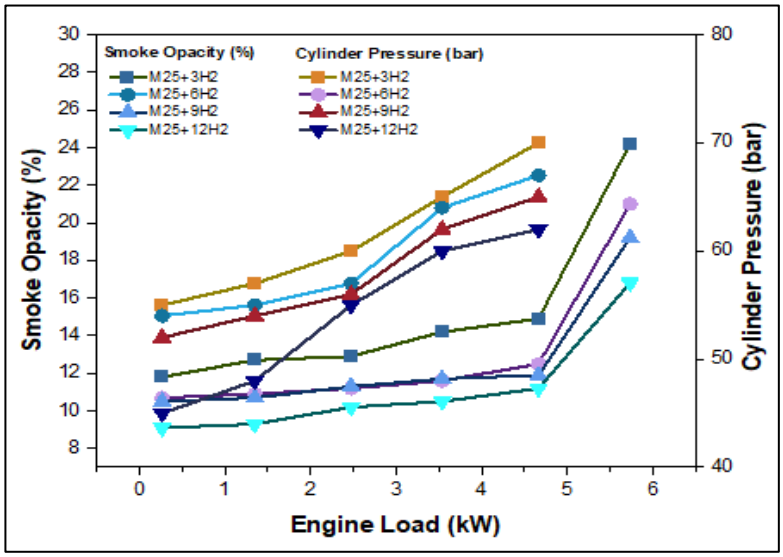

Figure 4: Smoke emission and cylinder pressure with varying engine loads.
Source: Authors, (2026).

Hydrogen enrichment influences smoke opacity and peak cylinder pressure for M25 gasoline across various engine loads, as illustrated in Figure 4. Increased hydrogen flow rates markedly reduce soot generation, illustrating hydrogen's role in enhancing combustion quality; yet, smoke opacity consistently increases with load across all mixes. Hydrogen's carbon-free characteristics reduce the carbon-to-hydrogen ratio and minimize particulate matter production, resulting in a decrease in opacity from 16.8% for M25+3H2 to 10.5% for M25+12H2 at low load (0 kW), and from 38 % to 25 % at maximum load (6 kW)—a reduction of 28% and 21%, respectively. Similarly, peak cylinder pressure escalates with load for all blends; additionally, hydrogen enrichment validates its combustion-enhancing function by further elevating these values. The maximum pressure for M25+12H2 escalates from 50 bar under no load to 58 bar under full load, reflecting a 16% enhancement, whereas for M25+3H2, it grows from 60 bar to 67 bar, indicating a 11.7% improvement. Collectively, these data indicate that the incorporation of hydrogen enhances engine performance by reducing smoke emissions and augmenting combustion intensity through elevated in-cylinder pressures. In previous studies, B20 mahua oil methyl ester–acetylene dual-fuel RCCI engine tested with acetylene injected at 60° at 1–5 lpm. Best at 4 lpm gave 32.6% BTE, slightly below conventional diesel, but reduced NOx (11.8%), smoke (10.4%), HC (5.3%), and CO (14.3%) [25].

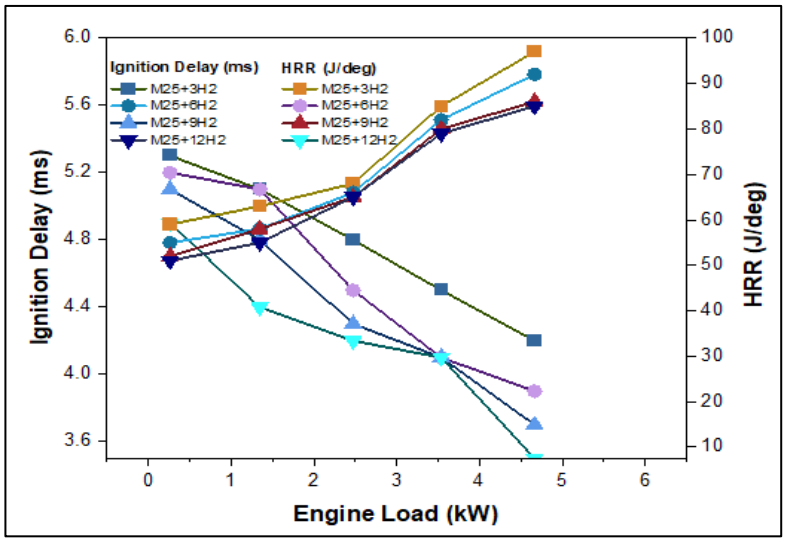

Figure 5: Ignition delay and HRR with varying engine loads.
Source: Authors, (2026).

Figure 5 illustrates the impact of varying engine loads and hydrogen enrichment levels on ignition delay and heat release rate (HRR) for M25 fuel at hydrogen flow rates of 3, 6, 9, and 12 lpm. As the load and hydrogen concentration rise, the ignition delay continuously diminishes, indicating enhanced fuel reactivity and increased combustion stability. Due to elevated in-cylinder temperatures and pressures, along with hydrogen's propensity to promote premature flame ignition, the duration drops from 5.3 ms to 4.6 ms (a reduction of 13.2%) at full load (5.0 kW) and from 3.8 ms for M25+3H2 to 3.3 ms (a reduction of 15.7%) at zero load. Furthermore, the heat release rate (HRR) consistently escalates with load across all blends, exhibiting a more pronounced association for those with elevated hydrogen enrichment. An increase in heat release rate (HRR) from 50 J/deg. for M25+3H2 to 58 J/deg. for M25+12H2 at zero load (a 16% increase) and from 86 J/deg. to 97 J/deg. (a 12.7% increase) indicates more rapid and concentrated combustion. The elevated calorific value, accelerated flame speed, and reduced ignition delay of hydrogen contribute to these improvements; these elements facilitate faster and more complete combustion, resulting in a more pronounced energy release within a shorter crank angle duration. In earlier study, Spirogyra Biodiesel (SBD30) algae biodiesel tested with 1–2% DTBP (Di-Tert-Butyl Peroxide) cetane booster in a diesel engine. DTBP shortened ignition delay (max 9.43°CA vs diesel 11.5°CA), cut CO by 53.8%, smoke by 28.8%, but BTE dropped up to 10.41% vs diesel. NO rose up to 24.9%; combustion improved with DTBP [26].

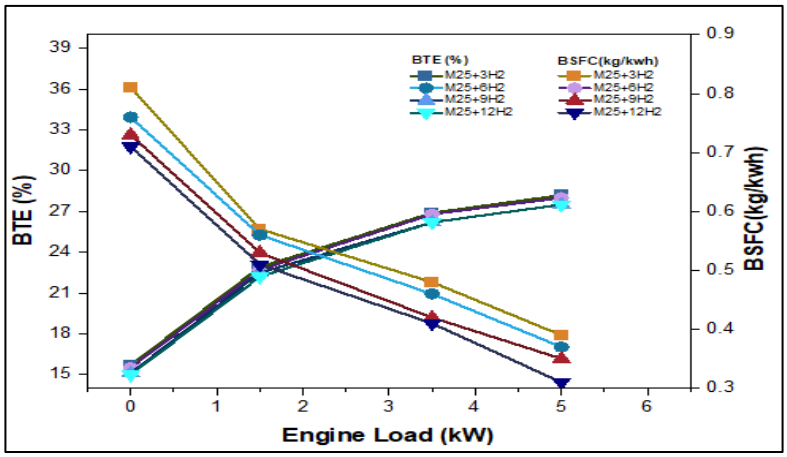

Figure 6: BTE and BSFC with varying engine loads.
Source: Authors, (2026).

Figure 6 illustrates the impact of injection timing on brake specific fuel consumption (BSFC) and brake thermal efficiency (BTE) for M25+12H2, considering various brake mean effective pressures (BMEP) and engine loads. As combustion efficiency increases with elevated loads, brake specific fuel consumption (BSFC) decreases with rising brake mean effective pressure (BMEP), irrespective of timing; nonetheless, injection timing significantly influences fuel consumption. The implementation of delayed injection enhances fuel-air mixing and optimizes the combustion efficiency of hydrogen, evidenced by a 13.5 % reduction in brake specific fuel consumption (BSFC) from 0.45 kg/kWh with IT21 to 0.30 kg/kWh with IT30 at 3.5 bar BMEP. The implementation of later timings such as IT27 and IT30 leads to diminished unburned fuel losses and enhanced mechanical efficiency, resulting in a more advantageous ignition delay for premixed combustion. This subsequently improves oxidation and produces elevated cylinder pressures at optimal crank angles. Similar to BTE, injection timing influences BTE; yet, improved combustion phasing yields more benefits from delayed injections. Peak pressure approaches top dead center (TDC) through timings such as IT30 and IT33, optimizing effective work production and reducing heat losses. The high diffusivity of hydrogen enhances homogeneous mixing and optimizes energy conversion efficiency. In another study, GO and ZnO nanoparticles (75 ppm) investigated in B20 mahua biodiesel with dispersant/surfactant. At 250 bar, BTE improved 5.067%, BSFC reduced 5.293%, NHRR up 43.50%. Emissions dropped: CO 11.07%, UHC 37.63%, NOx 27.77%, smoke 38.55%; ANN/RSM predictions highly accurate (R^2 = 0.93–0.99) [27].

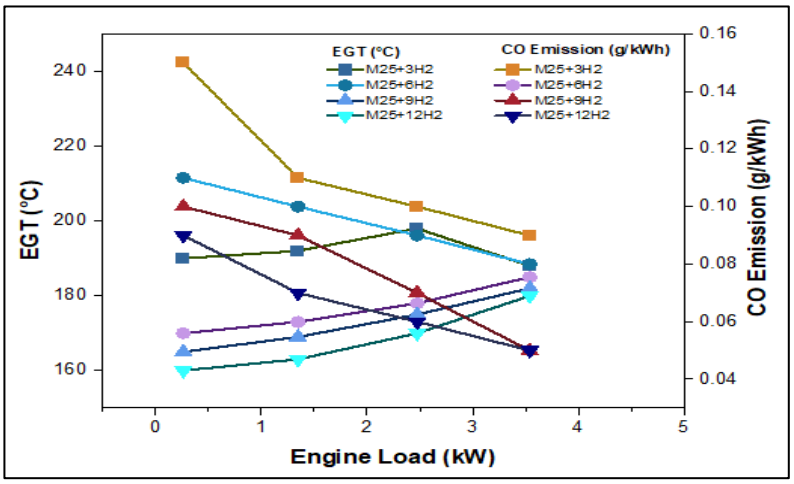

Figure 7: egt and co emission with varying engine loads.
Source: Authors, (2026).

For M25+12H2, Figure 7 illustrate the effect of injection timing on exhaust gas temperature and carbon monoxide emissions across various engine loads. Due to prolonged fuel combustion and elevated in-cylinder temperatures, exhaust gas temperature (EGT) consistently increases with load across all timings; however, delayed injection timing postpones the onset of combustion and shifts heat release nearer to the expansion stroke, resulting in a greater retention of energy in the exhaust. Despite elevated exhaust heat losses in IT33, the extended premixed combustion phase results in increased localized temperatures and higher exhaust gas temperatures (EGT), indicative of effective in-cylinder oxidation facilitated by hydrogen's rapid flame propagation. CO emissions, conversely, diminish as load escalates universally with subsequent injections yielding much reduced amounts. At low load (~1.5 kW), there is a 39.9 % reduction in CO emissions from 0.17 g/kWh for IT21 to 0.15 g/kWh for IT30, and a 37.5% reduction from 0.11 g/kWh to 0.07 g/kWh at full load (5.0 kW). Early combustion marked by reduced post-combustion temperatures that hinder CO oxidation to CO2, particularly at low loads, correlates with elevated CO levels at advanced timings such as IT21. Decreased CO emissions derive from enhanced mixing, maintained sufficiently high combustion temperatures, and increased oxidation efficiency, all of which transpire at later intervals.
Igure

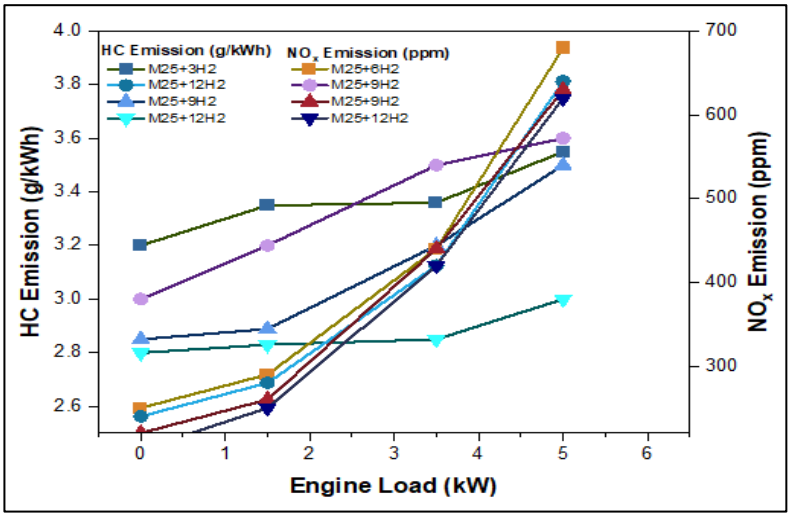

Figure 8: NOx and HC Emission with varying engine loads.
Source: Authors, (2026).

Figure 8 illustrate the impact of injection timing on the emissions of unburned hydrocarbons (HC) and nitrogen oxides (NOx) during M25+12H2 dual-fuel running at varying engine loads. Due to improved mixture preparation and enhanced combustion efficiency, hydrocarbon emissions consistently yield lower values with delayed injections; nonetheless, they steadily increase with load across all timings. At 1.5 kW, the hydrocarbon (HC) reduction is 15.2%, decreasing from 3.5 g/kWh with IT21 to 3.0 g/kWh with IT30; at 3.5 kW, the decrease is 10.2 %, down from 3.5 g/kWh to 2.0 g/kWh. The elevated hydrocarbon levels in advanced injection (IT21) result from premature combustion. This restricts the premixing duration and results in fuel pockets that are difficult to disperse, whereas delayed timings (IT27, IT30) permit extended premixing and leverage hydrogen's high diffusivity and broad flammability limits to enhance combustion uniformity. While NOx emissions diminish with successive injections, they escalate with load consistently. A reduction of 18.2% in NOx levels transpires at 1.5 kW, decreasing from 250 ppm (IT21) to 200 ppm (IT30), whilst an 10% reduction occurs at 650 kW, declining from 640 ppm (IT27) to 690 ppm (IT30). Advanced injection results in elevated in-cylinder temperatures and premature combustion, thereby enhancing thermal NOx production. Conversely, retarded injection augments cylinder volume at peak combustion, reduces flame temperature, and diminishes high-temperature residence time by aligning heat release with the expansion stroke. The results indicate that optimal performance and pollution management in dual-fuel engines can be attained by postponing injection timing, which successfully reduces HC and NOx emissions while balancing efficiency gains from hydrogen.

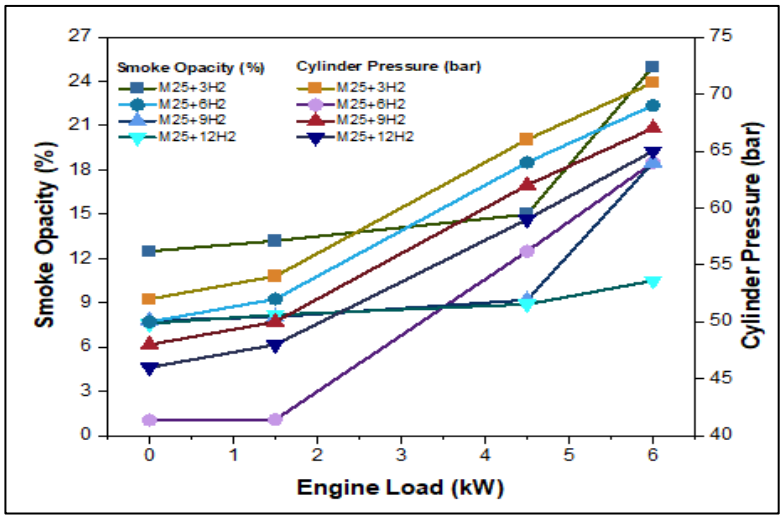

Figure 9: Smoke Opacity and Cylinder pressure with varying engine loads.
Source: Authors, (2026).

Figure 9 illustrate the impact of injection timing on smoke opacity and cylinder pressure for hydrogen-enriched M25 fuel blends under varying engine loads. Particulate emissions are significantly diminished by repeated injections; nonetheless, smoke opacity increases with load at all timings. A 22% decrease in opacity is observed at 1.5 kW with IT21 and 10.5% with IT30, however a 29.2% reduction is noted at 5.0 kW, decreasing from 26.2% to 21.5%. Advanced injection (IT21) leads to fuel-rich zones and heightened soot formation by decreasing the premixing duration, particularly under high load conditions. Conversely, delayed injection (IT27, IT30) enhances mixture homogeneity and leverages hydrogen's high diffusivity and carbon-free combustion to reduce smoke emissions. The pressure within the cylinder escalates in relation to the load consistently, with postponed injections leading to elevated maximum levels. An 8.7 % increase from 48 bar (IT21) to 59 bar (IT30) happens at 1.5 kW, whereas a 15 % increase from 64 bar to 69 bar occurs at 5.0 kW. This occurs because combustion is enhanced and in-cylinder energy release is optimized when injectors are delayed until the expansion stroke or near top dead center (TDC). This research demonstrates that hybrid fuel engines utilizing hydrogen exhibit reduced particle emissions and enhanced combustion intensity when employing strategic injection phasing, particularly IT30.

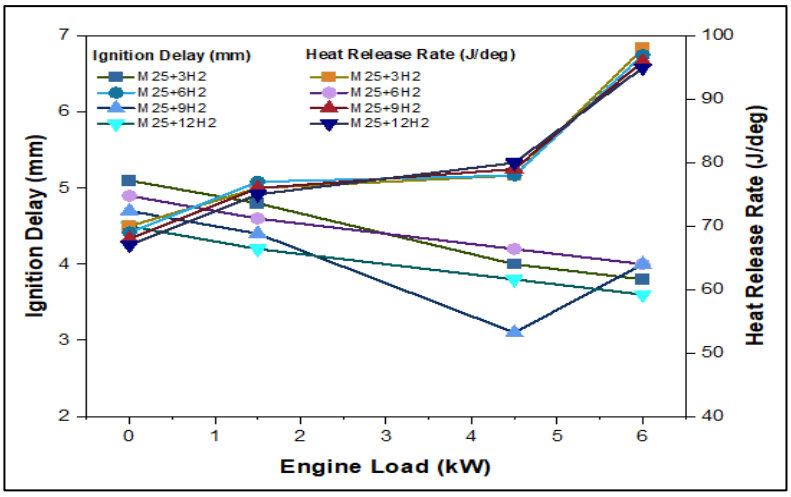

Figure 10: Ignition delay & HRR with load.
Source: Authors, (2026).

Figure 10 illustrate the impact of injection timing on ignition delay and heat release rate (HRR) for M25+12H2 fuel under varying engine loads. Ignition delay reliably diminishes with elevated load and delayed injection time, attributable to increase in-cylinder temperatures and pressures that enhance mixture reaction kinetics. At 1.5 kW, the duration decreases to 4.8 ms for IT30, reflecting a 9.3% reduction, while at 5.0 kW, it diminishes to 4.8 ms for IT30, indicating a 17.1% reduction. The responses increase with load consistently, but reaches its zenith at subsequent injections. An 8.2% increase transpires at 1.5 kW in HRR, rising from 67 J/deg. (IT21) to 75 J/deg. (IT30), while an 13.2% increase occurs at 5.0 kW, escalating from 76 J/deg. (IT24) to 98 J/deg. (IT30). The advantages of delayed injection timing in hydrogen-assisted dual-fuel operation are clearly shown in the progression of heat release rate (HRR). This mostly results from heavier loads elevating in-cylinder pressure and temperature, hence promoting accelerated combustion and enhanced energy release.

IV. RESPONSE SURFACE METHODOLOGY (RSM) ANALYSIS

Employing CCD, RSM was utilized to enhance the performance and emissions of the biodiesel-hydrogen dual-fuel engine. This study employed RSM to systematically assess and analyze the effects of IT and HFR on engine performance and emissions for optimal impact. The primary objective of employing RSM was to develop mathematical models capable of predicting BTE and NOx emissions. This would enable us to identify the optimal operating conditions. To minimize the number of experimental trials while preserving high model accuracy, CCD was employed to statistically evaluate interactions among variables. This method enabled the optimization of combustion in dual-fuel compression ignition engines by generating response surface plots that illustrated the trade-offs between efficiency and emissions. Brake Thermal Efficiency (BTE) and NOx emissions were selected as the primary responses to assess combustion efficiency and pollutant generation, while (IT) and (HFR) were considered as independent variables in the analysis. We developed a quadratic regression model for both responses and employed analysis of variance (ANOVA) to assess the significance of each component. This study assessed the built quadratic regression models for brake thermal efficiency (BTE) and NOx emissions by analyzing their goodness-of-fit. We assessed the model's predictive capability and dependability by computing the adjusted R2 and expected R2 values, representing the coefficient of determination (R2). An analysis of variance (ANOVA) was conducted to evaluate the statistical significance of each factor and their interactions. Significance was established as p values below 0.05. The models exhibited low residual errors and high R^2 values (>0.95), indicating their adequacy. The models were verified for homoscedasticity and normal distribution assumptions by diagnostic charts, including normal probability plots and residual vs predicted plots.

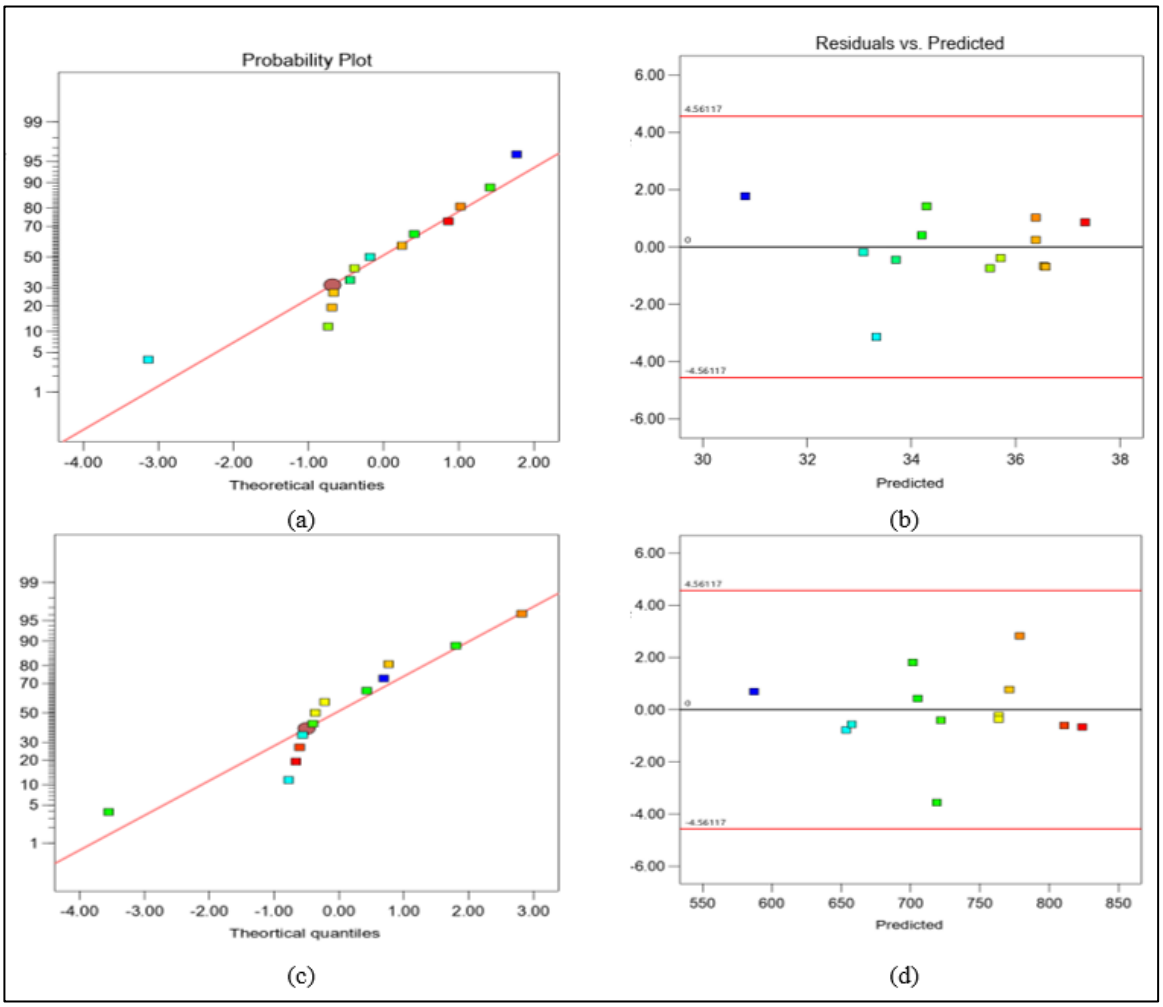

Figure 11: Response plots for model evaluation in (RSM): (a) normal probability plot of residuals for BTE (b) residuals versus predicted values for BTE (c) normal probability plot of residuals for NOx model, and (d) residuals versus predicted values for NOx. Source: Authors, (2026).

The analysis of variance (ANOVA) results for BTE indicate that the quadratic term (IT2) and injection timing (IT) significantly influence engine efficiency ($p<0.05$). The impact of Hydrogen Flow Rate (HFR) on the enhancement of Brake Thermal Efficiency (BTE) is somewhat significant ($p=0.0001$), indicating its role as a contributing factor. The results indicated no statistically significant interaction between IT and HFR ($p=0.0001$), suggesting that the two factors have independent rather than synergistic effects on BTE. Likewise, IT and IT2 emerged as the predominant contributors to NOx emissions, underscoring the significance of combustion phasing in NOx production. Injection timing, rather than fuel composition is the principal factor influencing NOx emissions, as hydrogen enrichment exerted a comparatively minor effect. The influence of injection timing and hydrogen flow rate on engine performance is illustrated in the 3D response surface plots for BTE and NOx.

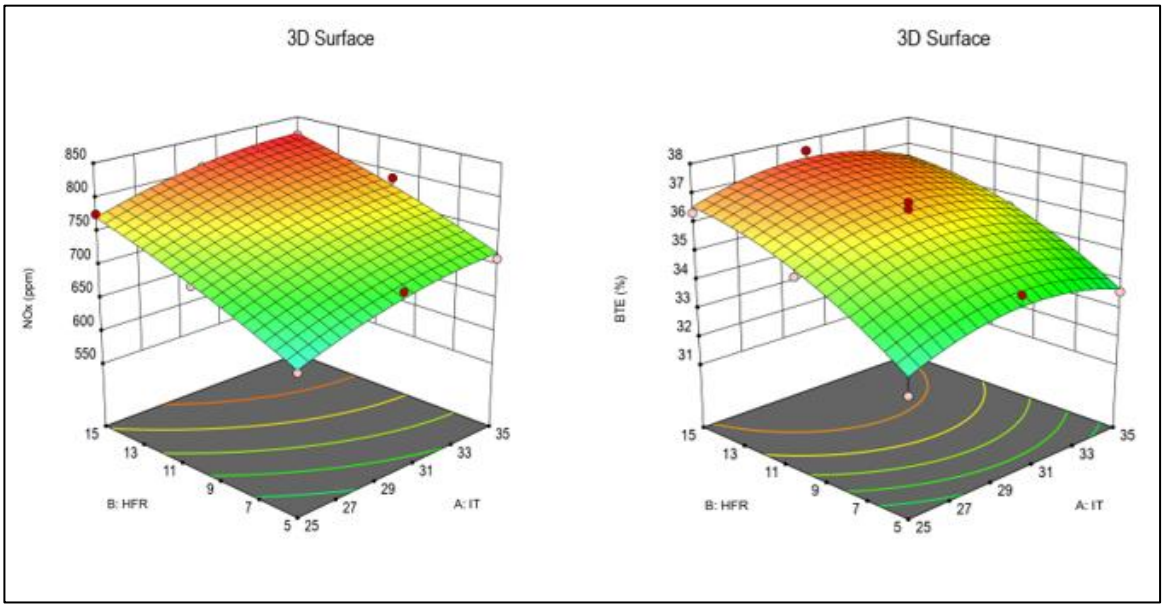

Figure 12: Response Surface for BTE., Response Surface for NOx.
Source: Authors, (2026).

Figure 12 illustrates that peak efficiency occurs between Injection Timings IT27 and IT28, with Brake Thermal Efficiency progressively rising from IT21 to IT27. Subsequent to this juncture, a minor decline is observed at IT30, perhaps because to excessive premixed combustion, resulting in increased heat dissipation. An elevated hydrogen enrichment (12 lpm) enhances combustion by augmenting flame speed and diffusivity, resulting in improved fuel-air mixing and complete combustion. The hydrogen flow rate is a significant parameter. The NOx emissions graph exhibits a clear rising trend as IT and HFR rise. It is confirmed that increased NOx production results from higher in-cylinder temperatures associated with hydrogen enrichment, with peak NOx formation occurring between IT27 and IT30 at an HFR of 12 lpm. There is a distinct necessity to employ after-treatment or exhaust gas recirculation (EGR) methods to mitigate NOx emissions without compromising efficiency, considering the inherent trade-off between the two. The results indicated that a projected BTE of 32.52% and nitrogen oxide (NOx) emissions of 751 ppm could be attained with an optimal injection timing of IT 27 and a hydrogen flow rate of 12 lpm, as established by the Response Surface Methodology (RSM) analysis. This signifies that this range encompasses the ideal configuration for attaining maximum efficiency with minimal emissions. Experimentation with EGR or SCR is necessary to alleviate the rise in NOx emissions. To further explore the influence of injection phasing on combustion temperature profiles and pollutant emissions, computational fluid dynamics (CFD) modeling may prove beneficial. Future research should examine the impact of reduced hydrogen flow rates (below 12 lpm) and optimize EGR ratios to attain a balance between combustion efficiency and regulatory NOx constraints. The RSM research indicates a significant enhancement in efficiency, with BTE attaining 32.52% with an advancement of injection timing to IT27 and an increase in hydrogen flow to 12 lpm. However, supplementary emission control strategies are necessary due to the increase in NOx emissions associated with it. An study of variance and response surface plots demonstrate that IT is superior to HFR, emphasizing the need of precise combustion timing.

V. CONCLUSION

A single-cylinder compression ignition engine utilizing M25 biodiesel and hydrogen was examined for its performance, combustion, and emission characteristics across various injection timings (IT21-IT30) and hydrogen flow rates (3-12 lpm). Experimental data indicate that injection time and hydrogen enrichment significantly influence engine efficiency and emission profiles. At a hydrogen flow rate of 12 lpm and an optimal IT27 configuration, the most favorable outcomes were attained at 5.8 bar BMEP, yielding BTE of 32.7% and brake-specific fuel consumption of 0.28 kJ/kWh. The heat release rate (HRR) of 98 J/deg and a peak cylinder pressure of 67 bar were attained at this setting, indicating enhanced combustion stability due to hydrogen's propensity to facilitate accelerated flame propagation. Emission studies of M25+12H2 at full load revealed a 54% reduction in CO emissions and a 24.7% reduction in HC emissions compared to M25+3H2. The efficacy of hydrogen in reducing particle generation was validated by a 37.2% reduction in smoke opacity. NOx emissions increased somewhat to 820 ppm, reflecting a 7.2% rise from the IT21 condition. These tendencies indicate that hydrogen enhances combustion efficiency while simultaneously elevating thermal NOx production due to increased cylinder temperature.

The optimal settings, identified by statistical optimization by Response Surface Methodology (RSM) were determined to be IT27.25˚ and 12 lpm, yielding a projected BTE of 32.52% and NOx emissions of 790 ppm. The elevated R2 values (>0.95) and the validation of the diagnostic plot confirmed the model's reliability. Future research should focus on integrating exhaust gas recirculation (EGR) or selective catalytic reduction (SCR) to mitigate NOx emissions. To evaluate thermal stress, material compatibility, and durability during hydrogen-assisted biodiesel combustion, it is recommended to conduct computational fluid dynamics (CFD) simulations and extended engine testing. These attempts could facilitate the implementation of M25-H2 dual-fuel systems, resulting in sustainable and policy-compliant transportation options.

VI. AUTHOR'S CONTRIBUTION

Conceptualization: Kumaran P, Sathiyaraj S.
Methodology: Kumaran P and Sathiyaraj S.
Investigation: Manivannan M and Rajasekar R.
Discussion of results: Kumaran P, Sathiyaraj S and Vijayakumar K.
Writing – Original Draft: Kumaran P.
Writing – Review and Editing: Sathiyaraj S and Vijayakumar K.
Resources: Kumaran P.
Supervision: Sathiyaraj S and Vijayakumar K.
Approval of the final text: Kumaran P, Sathiyaraj S and Vijayakumar K.

VII. REFERENCES

[1] S. Vellaiyan, S. Kuppusamy, D. Chandran, R. Raviadaran, and Y. Devarajan, "Optimisation of fuel modification parameters for efficient and greener energy from diesel engine powered by water-emulsified biodiesel with cetane improver," Case Studies in Thermal Engineering, vol. 48, 2023, doi: 10.1016/j.csite.2023.103129.

[2] A. Ahmad, A. K. Yadav, and A. Singh, "Biodiesel production from mahua oil: characterisation, optimisation, and modelling with a hybrid statistical approach," International Journal of Ambient Energy, vol. 44, no. 1, pp. 2618–2627, 2023, doi: 10.1080/01430750.2023.2262468.

[3] S. Balamurugan, D. Seenivasan, R. Rai, and A. Agrawal, "Optimization of biodiesel production process for mixed nonedible oil (processed dairy waste, mahua oil, and castor oil) using response surface methodology," Proceedings of the Institution of Mechanical Engineers, Part E: Journal of Process Mechanical Engineering, vol. 238, no. 2, pp. 862–874, 2024, doi: 10.1177/09544089221147392.

[4] B. Varadhan, C. A. Subasini, G. Palani, and M. Selvaraju, "Enhancing solar still distillation efficiency through integrated solar chimneys and submerged condenser systems," Thermal Science, vol. 28, no. 4, pp. 3155–3163, 2024, doi: 10.2298/TSCI230310122V.

[5] M. Udayakumar, S. Sivaganesan, and S. Sivamani, "Process optimization of KOH catalyzed biodiesel production from crude sunflower-mahua oil," Biofuels, vol. 13, no. 8, pp. 1031–1039, 2022, doi: 10.1080/17597269.2022.2071068.

[6] P. Raju, S. K. Masimalai, and N. Ganesan, "Extracting methyl-ester from waste cooking oil for fueling a light duty diesel engine–a dual fuel approach," Energy Sources, Part A: Recovery, Utilization and Environmental Effects, vol. 43, no. 12, pp. 1429–1443, 2021, doi: 10.1080/15567036.2019.1684602.

[7] A. Syed and S. M. Ali, "Enhancing Performance of Biodiesel–Hydrogen Blends Operated di Diesel Engine using dariable Injection Timing," Heat Transf Res, vol. 55, no. 2, pp. 1–20, 2024, doi: 10.1615/HeatTransRes.2023048573.

[8] V. S. Totad et al., "Hydrogen and Hydrogen-Blended Mahua Biodiesel Comparative Investigation in CI Engines Operating Under HCCI Combustion Mode with EGR Variation," Advances in Science, Technology and Innovation, vol. 2024, pp. 299–304, 2024, doi: 10.1007/978-3-031-63909-8_41.

[9] B. E. Samuel, S. Alghamdi, T. Priya, R. Deepalakshmi, S. Kannan, and M. Selvaraju, "Deep Learning-Driven Culvert Monitoring: A Novel Approach for Flash Flood Mitigation through Visual Blockage Analysis," in 2024 IEEE 9th International Conference for Convergence in Technology, I2CT 2024, 2024. doi: 10.1109/I2CT61223.2024.10543968.

[10] S. Muthuswamy and M. Veerasigamani, "Impact of secondary fuel injector in various distance on direct injection diesel engine using acetylene-bio diesel in reactivity controlled compression ignition mode," Energy Sources, Part A: Recovery, Utilization and Environmental Effects, vol. 46, no. 1, pp. 15220–15234, 2024, doi: 10.1080/15567036.2020.1810177.

[11] B. J. Bora et al., "Improving combustion and emission characteristics of a biogas/biodiesel-powered dual-fuel diesel engine through trade-off analysis of operation parameters using response surface methodology," Sustainable Energy Technologies and Assessments, vol. 53, 2022, doi: 10.1016/j.seta.2022.102455.

[12] V. Balan, S. Ramakrishnan, G. Palani, and M. Selvaraju, "Investigation on the Enhancement of heat transfer in counterflow double-pipe heat exchanger using Nanofluids," Thermal Science, vol. 28, no. 1A, pp. 233–240, 2024, doi: 10.2298/TSCI230312273V.

[13] P. Pradeep and M. Senthilkumar, "Simultaneous reduction of emissions as well as fuel consumption in CI engine using water and nanoparticles in Diesel - Biodiesel blend," Energy Sources, Part A: Recovery, Utilization and Environmental Effects, vol. 43, no. 12, pp. 1500–1510, 2021, doi: 10.1080/15567036.2019.1674958.

[14] S. Ramasubramanian, S. S. Kumar, L. Karikalan, and S. Baskar, "Performances emissions behaviors of Compression ignition engine by mahua oil," in Materials Today: Proceedings, 2020, pp. 982–985. doi: 10.1016/j.matpr.2020.06.187.

[15] S. K. Nayak et al., "Influence of injection timing on performance and combustion characteristics of compression ignition engine working on quaternary blends of diesel fuel, mixed biodiesel, and t-butyl peroxide," J Clean Prod, vol. 333, 2022, doi: 10.1016/j.jclepro.2021.130160.

[16] E. P. Venkatesan et al., "Performance and Emission Analysis of Biodiesel Blends in a Low Heat Rejection Engine with an Antioxidant Additive: An Experimental Study," ACS Omega, vol. 8, no. 40, pp. 36686–36699, 2023, doi: 10.1021/acsomega.3c02742.

[17] M. Tukaram Bai, U. Swarna, C. A. I. Raju, and V. Sridevi, "Production of methyl ester from mahua oil: Characterization and optimization by using RSM," in Materials Today: Proceedings, 2021, pp. 1609–1616. doi: 10.1016/j.matpr.2020.11.815.

[18] L. K. Prajapati, C. Tiwari, T. N. Verma, G. Dwivedi, and D. Paliwal, “Production and testing of mahua oil–based biodiesel synthesized through heterogeneous catalyst using experimental and numerical method,” Environmental Science and Pollution Research, vol. 31, no. 60, pp. 67280–67294, 2024, doi: 10.1007/s11356-024-33558-6.

[19] S. Swarna et al., “Biodiesel synthesis from mixed non-edible oil feedstock using K2CO3 in NH4OH Catalyst mixture,” Energy Sources, Part A: Recovery, Utilization and Environmental Effects, vol. 45, no. 3, pp. 6901–6917, 2023, doi: 10.1080/15567036.2023.2216163.

[20] Y.-G. Shen, K. Nie, J.-S. Xu, and G.-S. Chen, “Combustion and Emission Characteristics of Compression- Ignition Aero Piston Engine at Different Altitudes,” Tuijin Jishu/Journal of Propulsion Technology, vol. 43, no. 4, 2022, doi: 10.13675/j.cnki.tjjs.200896.

[21] H. E. Gülcan and M. Ciniviz, “The effect of pure methane energy fraction on combustion performance, energy analysis and environmental - economic cost indicators in a single-cylinder common rail methane-diesel dual fuel engine,” Appl Therm Eng, vol. 230, 2023, doi: 10.1016/j.applthermaleng.2023.120712.

[22] S. Pandey, S. S. Bhurat, and R. Kunwer, “Investigation of fumigation of ethanol and exhaust gas recirculation on combustion and emission characteristics of partially premixed charge compression-ignition engine,” Energy Sources, Part A: Recovery, Utilization and Environmental Effects, vol. 47, no. 1, pp. 4436–4450, 2025, doi: 10.1080/15567036.2020.1868625.

[23] D. K. Sahu, C. H. Patel, S. K. Uppara, S. Kanchan, and R. Choudhary, “Parametric evaluation of B20 blend of mahua biodiesel with nanomaterial additives,” in Materials Today: Proceedings, 2021, pp. 804–811. doi: 10.1016/j.matpr.2021.05.589.

[24] P. P. Kumar, S. Pendyala, and S. K. Gugulothu, “Multi-objective optimization of CRDI engine characteristics powered with Mahua methyl ester/diesel blend: a Taguchi fuzzy approach,” Environmental Science and Pollution Research, 2023, doi: 10.1007/s11356-023-28795-0.

[25] S. Muthuswamy and M. Veerasigamani, “Comparative experimental analysis on dual fuel with biodiesel-acetylene in reactivity controlled compression ignition engine,” International Journal of Ambient Energy, vol. 43, no. 1, pp. 6317–6328, 2022, doi: 10.1080/01430750.2021.2014958.

[26] A. Samraj, D. Barik, K. Tudu, P. Paramasivam, P. K. Kanti, and A. G. Ayanie, “Experimental Investigation on Spirogyra Biodiesel With Di-Tert-Butyl Peroxide as a Cetane Booster,” Energy Sci Eng, vol. 13, no. 6, pp. 3328–3341, 2025, doi: 10.1002/ese3.70105.

[27] S. R. Pala, M. V. K. Mohan, and V. S. P. Vanthala, “Optimizing performance, combustion and emission characteristics of mahua biodiesel included GO and ZnO nanoparticles: an ANN-RSM approach,” Environmental Science and Pollution Research, vol. 32, no. 23, pp. 14169–14201, 2025, doi: 10.1007/s11356-025-36530-0.